

Charge Controlled Swelling of Microgel Particles

A. Fernández-Nieves,[†] A. Fernández-Barbero,[†] B. Vincent,[‡] and F. J. de las Nieves^{*,†}

Group of Complex Fluids Physics, Department of Applied Physics, University of Almería, 04120 Almería, Spain, and School of Chemistry, University of Bristol, Cantock's Close, Bristol BS8 1TS, United Kingdom

Received September 8, 1999; Revised Manuscript Received November 30, 1999

ABSTRACT: The swelling of cationic microgel particles has been studied experimentally, in the weak screening regime. The solution pH was selected as the external variable triggering the swelling, which was followed by dynamic light scattering. The particle charge was determined by conductometric and potentiometric titrations, leading to a good correlation between the charge of the microgel network and its size. This leads to the conclusion that the swelling is mainly charge controlled. The Flory–Huggins thermodynamic theory for gels, including a term accounting for the counterion distribution within the microgel, has been used to interpret the experimental data. The osmotic term associated with the counterions explains fairly well the observed behavior, and additional contributions due to the internal microgel microscopic structure are not necessary, as Pincus et al. have suggested.

I. Introduction

A gel is a three-dimensional cross-linked polymer network immersed in a fluid.¹ Microgel particles are gels with dimensions in the colloidal range. These systems are currently the focus of considerable scientific research due to their potential technological application in a large number of areas: medicine, industry, biology, and environmental cleanup. Applications for such materials include rheological control for high solid formulations in the surface coating industry,² uptake and release of heavy metal ions,³ drug delivery,⁴ optoelectronic switches,⁵ and artificial muscles.⁶ The reason for such interest is because of their ability to respond reversibly to external stimuli, such as temperature, pH, ionic strength, solvent nature, and external stress, and also in certain cases because of their biocompatibility. Attention has also been paid to their synthesis and preparation as reviewed by Murray and Snowden,⁷ viscoelastic properties,^{8,9} swelling,^{10–12} and electrokinetic behavior.¹³ These novel gels show interesting features due to the superposition of intrinsic properties of gels and those of colloids.

From a more fundamental point of view, the properties of polyelectrolyte solutions and gels are not very well understood, and the elegant scaling theories that have been successfully developed for neutral polymers are not easily extended to charged systems. This is mainly due to the long-range character of the Coulomb interaction and to the effect of the counterion distribution.

The present paper deals with the swelling of poly(vinylpyridine) microgel particles. This system is an excellent model for studying the swelling of ionized polymer networks since the network contains pH-dependent ionizable groups. A slight pH variation can modify the network electrical charge, controlling the interaction between chains and, hence, the polymer-mesh dimensions. The particle size has been monitored

using dynamic light scattering. The surface and bulk particle charge densities were determined directly by conductometric and potentiometric titrations. A strong correlation between the charge and the particle volume was found, indicating that the microgel swelling is mainly controlled by the extent of charging of the network.

The Flory–Huggins-based thermodynamic theory has been used to discuss the experimental results. The model used accounts for the electrostatic contribution by including the effect of the counterions associated with the charges on the polymer network. As will be demonstrated, the osmotic term associated with the counterions explains fairly well the observed behavior, and additional contributions due to the internal microgel microscopic structure are not necessary.

The outline of the paper is as follows: section II is a summary of the theoretical background dealing with the thermodynamic description of the swelling in microgel particles; the experimental system and techniques are described in section III. Experimental results are reported, discussed, and compared with theoretical predictions in section IV. Finally, section V summarizes the conclusions.

II. Theoretical Background

Thermodynamic equilibrium for a gel is attained when the chemical potential of the solvent is equal inside and outside the gel, that is, when no net transfer of solvent takes place across the gel–solvent interface.¹⁴ Thus, the osmotic pressure within a gel must be zero once equilibrium is reached.

The macroscopic state of a homogeneous, neutral gel may be described through the total osmotic pressure inside the gel, which consists of two terms: a mixing contribution and an elastic component. The mixing and elastic osmotic pressures, π_m and π_e , are given by the Flory theory:¹⁵

$$\pi_m = - \frac{N_A k T}{v_s} [\phi + \ln(1 - \phi) + \chi \phi^2] \quad (1)$$

[†] University of Almería.

[‡] University of Bristol.

* Corresponding author. e-mail: fjnieves@ualm.es.

$$\pi_e = \frac{N_C k T}{V_0} \left[\left(\frac{\phi}{2\phi_0} \right) - \left(\frac{\phi}{\phi_0} \right)^{1/3} \right] \quad (2)$$

where N_A is the Avogadro constant, k the Boltzmann constant, T the temperature, and v_s the molar volume of the solvent. ϕ_0 and V_0 are the volume fraction of polymer and volume of the microgel particle in the unswollen state, respectively. ϕ is the volume fraction of polymer in the swollen gel. N_C stands for the effective number of chains, and χ is the Flory polymer-solvent interaction parameter. When χ is reduced below 0.5, a polymer chain changes from a compact globule to an extended coil. Similarly, a gel network changes from the swollen to the collapsed states. Thus, the equilibrium conditions may be externally modified through control of the solvency parameter, which is sensitive to the temperature, solvent composition, and other variables.

In the case of ionized polymer networks, an additional term accounting for the repulsion between polymer chains has to be considered. Two different, but closely related, standpoints have usually been adopted for treating this problem. In the first, the effect of the charges forming part of the network is considered. These exert marked Coulombic repulsion which tends to expand the polymer chains. The other approach concentrates on the effect of counterions, which give rise to an extra osmotic pressure (Donnan effect), which also tends to expand the network.¹⁵

Let us consider a macroscopic polyelectrolyte gel, in a salt-free medium and whose charge density is smaller than the value at which Manning condensation^{16–19} may take place, so that the Debye-Hückel linear screening approximation is valid. The contribution to the osmotic pressure due to the presence of the counterions may then be expressed as^{14,20,21}

$$\pi_i = \frac{f N_C k T}{V_0} \frac{\phi}{\phi_0} \quad (3)$$

where f is the number of counterions per polymer chain.

The number of chains in eqs 2 and 3 may be estimated, for a chemically cross-linked copolymer comprised of monomers A and B, with A being present at a lower concentration than B, by the following expression:²²

$$N_c = 2N_A X = 2N_A \frac{V_0 \rho_b}{M_a + \left(\frac{1}{x_a} - 1 \right) M_b} \quad (4)$$

where X stands for the moles of cross-links; ρ_b , M_a , M_b , and x_a are the density, molecular weight, and mole fraction of monomer A or B, as indicated.

The equilibrium condition, $\pi_{\text{total}} = \pi_m + \pi_e + \pi_i = 0$, is given (from eqs 1–3) by

$$\phi + \ln(1 - \phi) + \chi \phi^2 - \frac{N_c v_s}{N_A V_0} \left[f + \frac{1}{2} \left(\frac{\phi}{\phi_0} \right) - \left(\frac{\phi}{\phi_0} \right)^{1/3} \right] = 0 \quad (5)$$

Assuming that the swelling is isotropic, the following relationship between the diameter of a spherical microgel particle and the average polymer volume fraction

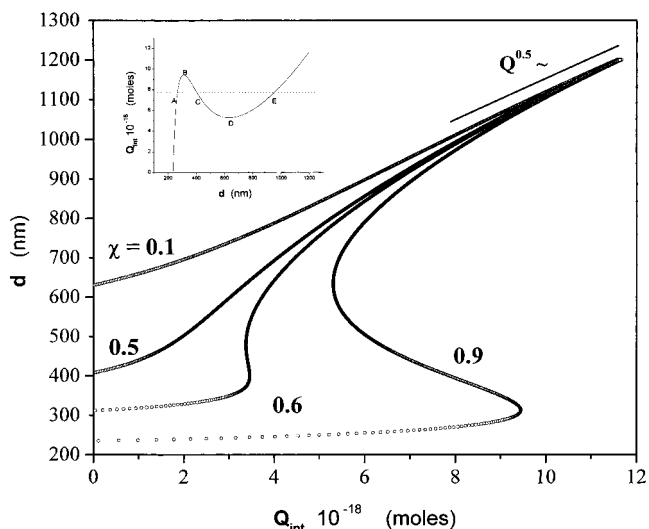


Figure 1. Swelling plot of a microgel according to the Flory-Huggins thermodynamic model for different values of χ . d is the particle diameter, and Q_{int} is the number of fixed charges per particle, which equals the number of counterions. $d_0 = 200$ nm; $\phi_0 = 1$. Cross-linker concentration = 0.25 wt %. In the upper-left-hand corner the curve for $\chi = 0.9$ is plotted, in an alternative form.

within it holds:

$$\frac{\phi}{\phi_0} = \frac{V_0}{V} = \left[\frac{d_0}{d} \right]^3 \quad (6)$$

where d_0 and d are the collapsed and swollen diameters, respectively.

An example of the microgel swelling behavior as a function of the charge on the particle is shown in Figure 1 for different χ values. The number of counterions is equal to the number of charges on the polymer chains, $Q_{\text{int}} = f N_C$. The curve shape strongly depends on the value of χ . For low charge, the mixing and elastic terms dominate the osmotic pressure. A strong dependence of the swelling on the solvency parameter is seen since χ controls the mixing contribution (eq 1). As χ increases, the solvent-polymer contacts are less favored than the polymer-polymer contacts and the particle deswells. For low χ values, the size increases monotonically with the number of counterions. In the case of higher χ values, the curve indicates two coexisting particle sizes for a given Q_{int} value. To clarify this point in an alternative form, the particle charge is plotted as a function of the particle size for $\chi = 0.9$, in the upper-left-hand corner. Let us consider for discussion the ionized gel with 8×10^{-18} mol of counterions (dotted line). The two possible equilibrium particle sizes are indicated by points A and E. Hence, for high χ values, a phase transition is expected for the ionized microgel. Below this value, the microgel experiences a continuous change between the collapsed and swollen phases, and thus, no first-order phase transition occurs.

For higher Q_{int} values, the curve becomes χ independent as expected, since the electrical and elastic terms dominate over the mixing one. In this case, the asymptotic behavior $d \sim Q^{0.5}$ becomes apparent. This predicted asymptotic trend will be one of the points experimentally tested in this paper using an ionizable microgel.

III. System and Methods

Experimental System. Cationic microgel particles were employed in this work for testing the swelling model previously

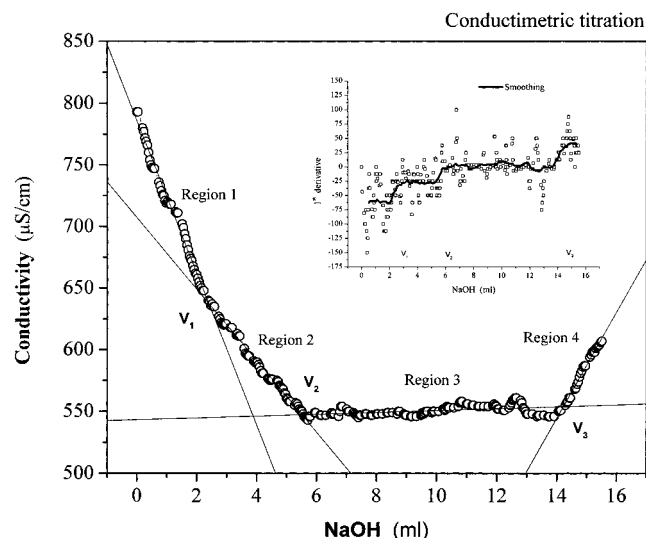


Figure 2. Conductometric titration of the microgel particles.

described. The synthesis of the microgel particles is described elsewhere.²³ They were based on poly(2-vinylpyridine) (2VP), cross-linked with divinylbenzene (DVB, 0.25 wt %). The initiator used was 2,2'-azobis(2-amidinopropane) dihydrochloride (V50, Wako).

Two types of groups are able to confer charge to the colloidal particles: (i) amidinium groups arising from the initiator, located essentially at the periphery of the particles, and (ii) the constituent monomer 2VP, which is expected to be uniformly distributed throughout the bulk of the particles. The pK_a of 2VP is 5, and that of the amidinium groups is around 10.²⁴ The DVB is also expected to be homogeneously distributed throughout the particles. Hence, a polyelectrolyte-type particle model is more realistic than a core-shell structure.

Transmission electron microscopy (TEM) showed the particles to be spherical and highly monodisperse, with a diameter of 205 ± 8 nm.²³

In summary, the particles will be considered as spherical polyelectrolytes, homogeneously cross-linked, with pH-dependent charge groups, both on their surface and inside their volume.

Experimental Methods. The total charge per microgel particle was determined by both conductometric and potentiometric titrations. These experiments were carried out in a cell that supported the pH or conductivity electrode, a nitrogen inlet tube, and a sodium hydroxide or hydrochloric acid feed tube, controlled with a dispenser of ± 1 μ L sensitivity. The microgel dispersion was stirred during the titration, the data being collected by a computer.

The average hydrodynamic diameter of the microgel particles was determined by dynamic light scattering (4700, Malvern Instruments). Dispersions were prepared at a concentration of 5×10^9 particles cm^{-3} , adjusting the ion concentration to 1 mM NaCl.

IV. Results and Discussion

Particle Charge. Conductometric titrations were performed in order to determine the total surface and bulk charges. In addition, charging and discharging potentiometric titrations were carried out to obtain the charge pH dependence.

Figure 2 shows a conductometric titration where four regions may be distinguished. This titration may be described as a "discharging" titration, since, at the starting point, pH = 3, essentially all the groups are protonated. The values of V_1 , V_2 , and V_3 were identified with the positions of the discontinuities appearing in the derivative of the experimental curve (right-upper-hand corner). The four regions labeled in the graph

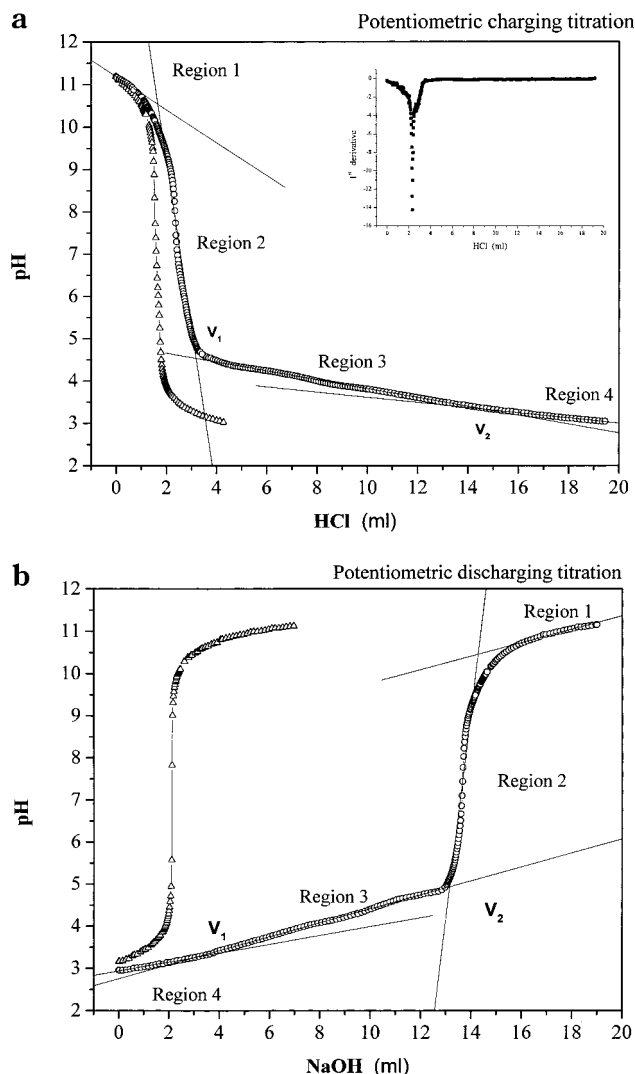


Figure 3. (a) Potentiometric charging titration of the microgel particles and the reference curve: \blacktriangle , NaOH (reference); \circ , microgel + NaOH. (b) Potentiometric discharging titration of the microgel particles and the reference curve: \blacktriangle , HCl (reference); \circ , microgel + HCl.

characterize the initial excess of H^+ ions (region 1), neutralization of amidinium groups (region 2), the titration of 2VP groups (region 3), and the excess of OH^- ions (region 4). The following charge values were obtained: $Q_s = (3.6 \pm 0.4) \times 10^{-18}$ mol of charges/particle for the surface amidinium groups and $Q_{\text{int}} = (1.30 \pm 0.15) \times 10^{-17}$ mol of charges/particle for the vinylpyridine groups which constitute the polymer network. These values were based on the volume differences $V_3 - V_2$ (bulk charge) and $V_2 - V_1$ (surface charge).

Figures 3 shows the charging and discharging potentiometric titrations of the microgel particles, as well as the reference curves corresponding to the titration solutions, NaOH and HCl. Figure 3a is the charging titration, starting at pH = 11 where all the ionizable groups are deprotonated. The same four regions as those appearing in the conductometric titration (Figure 2) may also be distinguished here. It is of interest to note that the reference and microgel data coincide in the initial part for both curves, indicating that the particles do not consume the added protons in this region. The second region ends at pH. 4.8. The charging of the amidinium groups takes place in this region. From the

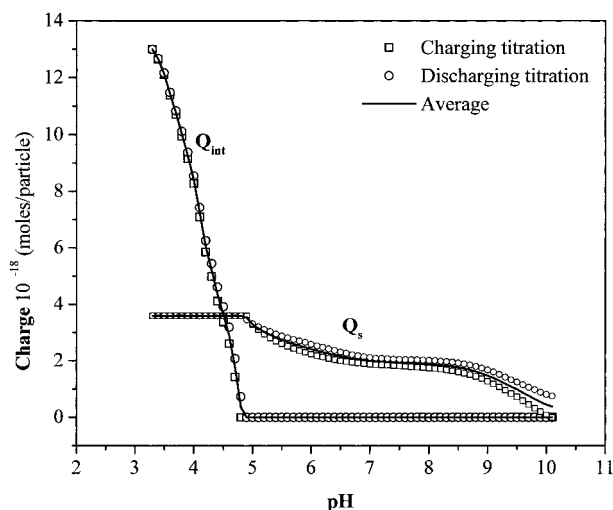


Figure 4. Surface charge (Q_s) and polymer network charge (Q_{int}) of a microgel particle versus pH. The results from charging and discharging titrations are shown, as well as their average that is used as the actual charge.

difference between the microgel and reference curves, the surface charge as a function of pH is extracted. In the third region, the titration of the 2VP groups occurs. The fourth region starts at pH. 3.3, corresponding to the excess of OH^- ions (region 4 in Figure 2). The surface charge was obtained from the analysis of the peak width of the first derivative, plotted in the right-upper corner of Figure 3a. On the other hand, the amount of HCl employed for the network groups tritration was extracted from the difference between volumes V_1 and V_2 .

The discharging potentiometric titration is shown in Figure 3b. The total surface and volume charges were obtained as previously described for the charging potentiometric titration. The charge pH dependence was also determined from the difference between the microgel and reference curves, yielding the amount of charge neutralized with respect to the total charge.

Finally, the charge–pH curves from the charging and discharging potentiometric titrations are shown in Figure 4. Good agreement between both data sets is observed. As expected, the surface charge, Q_s , increases as the pH decreases, due to the ionization of the amidinium groups. However, the bulk charge, Q_{int} , begins to appear below pH 4.8 when the 2VP groups start to protonate.

Particle Size. Figure 5 shows the mean hydrodynamic diameter, $\langle D \rangle$, as a function of the pH. The particle swelling starts below about pH 4.2, a value which is slightly lower than the one for which the polymer network starts charging (pH = 4.8). Above pH 4.2, the particles are in the deswollen state because of the absence of inner charge, having a mean diameter in this state of 230 ± 15 nm. Additional measurements were carried out at higher pHs (not plotted in Figure 5), but as expected, no changes in the particle size were observed. It is interesting to point out that this value is close to the TEM particle size 205 ± 8 nm, but not exactly the same. In the “dry state” the particle size is slightly smaller than in the case of the nonionized network in water. This is consistent with the observation of Figure 1, that in absence of charge ($Q_{int} = 0$), the mixing contribution to the osmotic pressure expands the polymer mesh. Thus, the particle size (in absence of charge) depends strongly on the χ solvency parameter

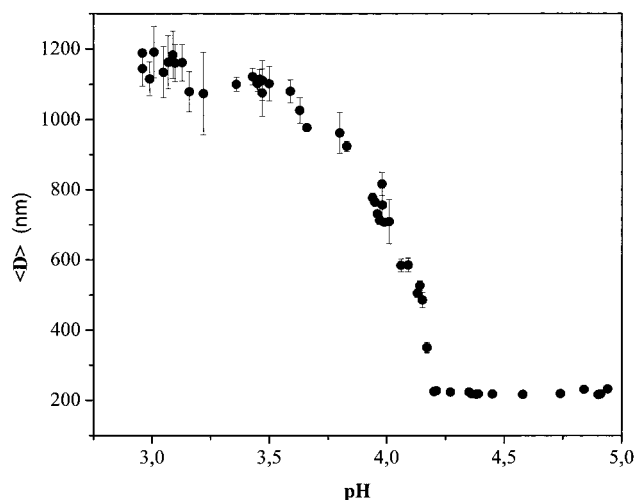


Figure 5. Experimental mean hydrodynamic diameter versus pH.

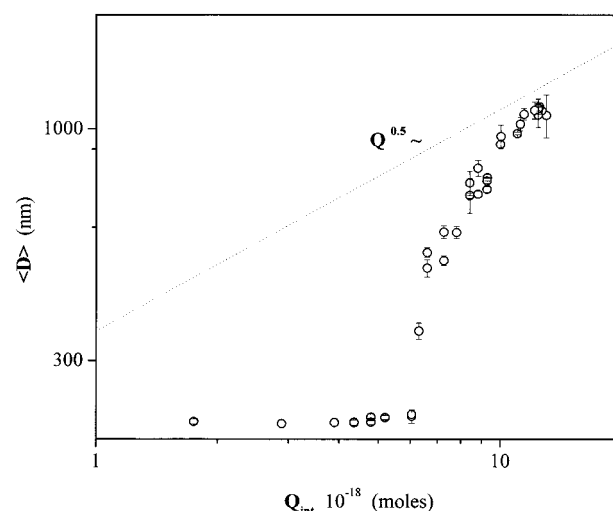


Figure 6. Experimental mean hydrodynamic diameter versus calculated polymer network charge.

through the mixing term. In the case plotted in Figure 1, the collapsed particle size was set at 208 nm, while the calculated for $Q_{int} = 0$ and $\chi = 0.6$ is 300 nm.

When the charge increases abruptly due to the protonation of the 2VP groups (Figure 4), the microgel swells. Below this transition pH, the polymer network becomes increasingly more ionized, and the particle volume increases. Close to the transition pH (see Figure 5), the swelling is very strong because the electrical term (linear with the volume fraction in the equilibrium equation) controls the swelling at large ϕ values (small particle size). However, for lower pHs, the term $\phi^{1/3}$ of the elastic contribution dominates (large particle size), despite the high value of the charge network, f . This implies that the swelling becomes less steep, as may be observed in Figure 5.

Finally, it is of interest to note that the surface charge itself does not influence the particle size, contributing only to the dispersion stability through electrical repulsion between particles.

Charge-Controlled Swelling. Figure 6 shows the experimental correlation between the mean particle diameter and the polymer network charge. The swelling increases slightly for particle charge lower than a critical value (around 6×10^{-18} mol). In other words, even in the presence of charge, the microgel maintains

its collapsed size. This aspect has already been noted from the differences in the pH values at which the polymer network starts charging (pH = 4.8) and for which the microgel actually starts to swell (pH = 4.2). This interesting finding is qualitatively described by the model (Figure 1), which also predicts a transition region, where an insensitivity of the particle size to the network charge occurs.

Above the critical charge value, any further increase of Q_{int} causes a strong increase in particle size. The experimental swelling occurs continuously from the deswollen to the swollen state. No discontinuous transition was observed, implying a value for the Flory parameter below 0.6. (Figure 1).

For even higher Q_{int} values, the swelling rate decreases, corresponding to the asymptotic behavior, with an scaling exponent 0.5, as predicted by the theory (see Figure 1). This indicates once again that the swelling process is controlled by the counterion contribution to the osmotic pressure. Therefore, when the mesh size of the gel is smaller than the Debye length, in the weak screening limit, the swelling of the microgel is driven by the osmotic pressure of the counterions. This pressure acts on the boundary of the gel and creates a tension transmitted to the internal chains through the cross-links. The chains of the gel behave therefore as isolated chains stretched by an external force, and additional contributions due to the internal microgel structure are not really relevant, as Pincus et al. theoretically demonstrated.^{25,26}

V. Conclusions

The volume phase transition of charged microgel particles under weak screening conditions was found to be continuous and controlled by the extent of charging of the particles. An initial insensitivity of the particle size with the charge was found as well as an asymptotic behavior $d \sim Q^{0.5}$, for large Q values. The relation between the charge and the particle size has been explained with the Flory–Huggins thermodynamic model for gels, including only the effect of the counterion distribution caused by the presence of fix charges on the microgel network.

Acknowledgment. The authors thank Dr. A. Loxley for the particle synthesis. A.F.N. expresses his gratitude to the Ministerio de Educación y Cultura for granting a stay at the University of Bristol. This work was supported by Comisión Interministerial de Ciencia y Tecnología under project MAT 96-1035-C03-03 and by Acción Integrada Hispano-Británica (HB 1998-0225).

References and Notes

- (1) Tokita, M.; Tanaka, T. *J. Chem. Phys.* **1991**, *95*, 4613.
- (2) Quadrat, O.; Snuparek, J. *Prog. Org. Coat.* **1990**, *18*, 207.
- (3) Morris, G. M.; Vincent, B.; Snowden, M. J. *J. Colloid Interface Sci.* **1997**, *190*, 198.
- (4) Peppas, N. A. *Curr. Opin. Colloid Interface Sci.* **1997**, *2*, 531.
- (5) Sawai, T.; Yamazaki, S.; Ikariyama, Y.; Aizawa, M. *J. Electroanal. Chem.* **1991**, *297*, 399.
- (6) Kajiwar, K.; Rossmurphy, S. B. *Nature* **1992**, *355*, 208.
- (7) Murray, M. J.; Snowden, M. J. *Adv. Colloid Interface Sci.* **1995**, *54*, 73.
- (8) Hirotsu, S. *J. Chem. Phys.* **1991**, *94*, 3949.
- (9) Tanaka, T.; Hocker, L. O.; Benedek, G. B. *J. Chem. Phys.* **1973**, *59*, 5151.
- (10) Hirotsu, S. *Macromolecules* **1992**, *25*, 4445.
- (11) Kato, E. *J. Chem. Phys.* **1997**, *106*, 3792.
- (12) Ohmine, I.; Tanaka, T. *J. Chem. Phys.* **1982**, *77*, 5725.
- (13) Ohshima, H. *Adv. Colloid Interface Sci.* **1995**, *62*, 189.
- (14) Hirotsu, S. *Phase Transitions* **1994**, *47*, 183.
- (15) Flory, P. J. *Principles of Polymer Chemistry*; Cornell University Press: London, 1953.
- (16) Manning, G. S. *Acc. Chem. Res.* **1979**, *12*, 443.
- (17) Manning, G. S. *Physica A* **1996**, *231*, 236.
- (18) Levin, Y.; Barbosa, M. C.; Tamshiro, M. N. *Europhys. Lett.* **1998**, *41*, 123.
- (19) Fernández-Nieves, A.; Fernández-Barbero, A.; de las Nieves, F. J. *Langmuir*, accepted.
- (20) Barrat, J. L.; Joanny, J. F.; Pincus, P. *J. Phys. II* **1992**, *2*, 1531.
- (21) Tanaka, T.; Sato, E.; Hirokawa, Y.; Hirotsu, S.; Peetermans, J. *Phys. Rev. Lett.* **1985**, *55*, 2455.
- (22) Saunders, B. R.; Vincent, B. *Colloid Polym. Sci.* **1997**, *275*, 9.
- (23) Loxley, A.; Vincent, B. *Colloid Polym. Sci.* **1997**, *275*, 1108.
- (24) Perrin, D. D. *Dissociation Constants of Organic Bases in Aqueous Solution*; Butterworths: London, 1965.
- (25) Barrat, J. L.; Joanny, J. F.; Pincus, P. *J. Phys. II* **1992**, *2*, 1531.
- (26) Pincus, P. *Macromolecules* **1997**, *24*, 2912.

MA991520L